Further Observation of the Tilted Planet XO-3: A New Determination of Spin-orbit Misalignment, a Possible Third Body, and Limits on Differential Rotation*

Teruyuki HIRANO,[1,2] Norio NARITA,[3] Bun'ei SATO,[4] Joshua N. WINN,[2] Wako AOKI,[3] Motohide TAMURA,[3] Atsushi TARUYA[1] and Yasushi SUTO[1,5]

hirano@utap.phys.s.u-tokyo.ac.jp

[1] *Department of Physics, The University of Tokyo, Tokyo, 113-0033, Japan*

[2] *Department of Physics, and Kavli Institute for Astrophysics and Space Research, Massachusetts Institute of Technology, Cambridge, MA 02139, USA*

[3] *National Astronomical Observatory of Japan, 2-21-1 Osawa, Mitaka, Tokyo, 181-8588, Japan*

[4] *Department of Earth and Planetary Sciences, Tokyo Institute of Technology, 2-12-1 Ookayama, Meguro-ku, Tokyo 152-8551*

[5] *Department of Astrophysical Sciences, Princeton University, Princeton, NJ 08544, USA*

(Received 2011 August 7; accepted)

Abstract

We report on observations of the Rossiter-McLaughlin (RM) effect for the XO-3 exoplanetary system. The RM effect for the system was previously measured by two different groups, but their results were statistically inconsistent. To obtain a decisive result we observed two full transits of XO-3b with the Subaru 8.2-m telescope. By modeling these data with a new and more accurate analytic formula for the RM effect, we find the projected spin-orbit angle to be $\lambda = 37.3^\circ \pm 3.0^\circ$, in good agreement with the previous finding by Winn et al. (2009). In addition, an offset of ~ 22 m s^{-1} was observed between the two transit datasets. This offset could be a signal of a third body in the XO-3 system, a possibility that should be checked with future observations. We also attempt to search for a possible signature of the stellar differential rotation in the RM data for the first time, and put weak upper limits on the differential rotation parameters.

Key words: stars: planetary systems: individual (XO-3) — stars: rotation — techniques: radial velocities — techniques: spectroscopic —

* Based on data collected at Subaru Telescope, which is operated by the National Astronomical Observatory of Japan.

1. Introduction

Since the discovery of the first transiting planet, many groups have been studying the stellar obliquities (spin-orbit angles) of planet-hosting stars through measurements of the Rossiter-McLaughlin (RM) effect. The RM effect is a distortion of stellar spectral lines that occurs during transits, originating from the partial occultation of the rotating stellar surface. It is often manifested as a pattern of anomalous radial velocities (RVs) during a planetary transit (Rossiter 1924; McLaughlin 1924; Queloz et al. 2000; Ohta et al. 2005; Winn et al. 2005; Narita et al. 2007; Triaud et al. 2010). By modeling the RM effect, one can determine the angle λ between the sky projections of the stellar rotational axis and the orbital axis. The statistics of the misalignment angle λ should provide a clue to the formation and evolution of close-in giant planets (hot-Jupiters and hot-Neptunes). Since 2008, many transiting systems with significant spin-orbit misalignments have been reported (e.g. Hébrard et al. 2008; Narita et al. 2009b; Pont et al. 2010). This has attracted much attention to the importance of dynamical mechanisms for producing close-in planets, as well as tidal evolution of planets and their host stars (Fabrycky & Tremaine 2007; Wu et al. 2007; Nagasawa et al. 2008; Chatterjee et al. 2008; Triaud et al. 2010; Winn et al. 2010).

In this paper, we present the measurement of the RM effect for the XO-3 system. The XO-3 system was discovered by Johns-Krull et al. (2008). Photometric follow-ups by Winn et al. (2008) allowed the system parameters to be refined. The large mass of the planet ($M_p = 11.79 \pm 0.59 M_{\rm Jup}$) and its eccentric orbit ($e = 0.260 \pm 0.017$) attracted further interest in this system.

Hébrard et al. (2008) detected the RM effect with the SOPHIE instrument on the 1.93 m telescope at Haute Provence Observatory (OHP). They found $\lambda = 70^\circ \pm 15^\circ$, suggesting a significant misalignment between the stellar spin axis and the planetary orbital axis for the first time among the known planetary systems. On the other hand, Winn et al. (2009) independently measured the RM effect with the High Resolution Echelle Spectrometer (HIRES) installed on the Keck I telescope, and found $\lambda = 37.3^\circ \pm 3.7^\circ$, which differs by more than 2 σ from the former result.

The reason for the discrepancy was unclear, but it may indicate the presence of unknown systematic errors in one of the datasets, or even in both. It is equally possible that the discrepancy should be ascribed to the different techniques adopted in modeling the RM effect. Hébrard et al. (2008) and Winn et al. (2009) both used analytic formulas to compute the anomalous velocity, but the former group used a formula that was based on a calculation of the first moment of the distorted line profile, while the latter group used a formula that was calibrated by numerical analysis of simulated RM spectra. Recently Hirano et al. (2011) presented a new and more accurate analytic formula for the RM effect, showing in particular that the RM velocity anomaly depends on many factors such as the rotational velocity of the

star, the macroturbulent velocity, and even the instrumental profile (IP) of the spectrograph, not all of which were considered in the previous literatures.

Specifically, for rapidly rotating stars like XO-3, the velocity anomaly calculated by Hirano et al. (2011) differs strongly from the simpler, previous analytic descriptions based on the first-moment approach (Ohta et al. 2005; Giménez 2006). When the incorrect relation is used between the RM velocity anomaly and the position of the planet, the results for λ may be biased.

In order to resolve the disagreement, and obtain a decisive result for the angle λ with fewer systematic errors, we observed another two full transits of XO-3b with the High Dispersion Spectrograph (HDS) on the Subaru 8.2-m telescope. We also applied the new analytic formula by Hirano et al. (2011) to model the RM effect with greater accuracy. We find that the best-fit value for λ based on our new measurements is very close to that reported by Winn et al. (2009).

We describe the detail of the observation in Section 2. The data analysis procedure and the derived parameters are presented in Section 3. Section 4 discusses the comparison with the previous results, and considers the possible effect of the stellar differential rotation.

2. Observations

We observed two complete transits of XO-3b with Subaru/HDS on November 29, 2009 and February 4, 2010 (UT). We also obtained several *out-of-transit* spectra on each of those two nights as well as on January 15, 2010 (UT). The out-of-transit spectra were obtained in order to help establish the Keplerian orbital parameters of the system. We adopted a typical exposure time as 600-750 seconds, and chose the slit width as $0.4''$, corresponding to the spectral resolution of $\sim 90,000$. We used the Iodine cell for precise RV calibration.

We reduced the images to one-dimensional (1D) spectra using standard IRAF procedures. The typical signal-to-noise ratio was $\sim$100 per pixel in the 1D spectra. We then processed the reduced spectra with the RV analysis routines for Subaru/HDS developed by Sato et al. (2002). Table 1 gives the resulting RVs and the associated errors, after correcting for the motion of the Earth. The quoted error is computed from the dispersion of RVs that were determined from individual 4 Å segments of the spectrum (Sato et al. 2002). We obtained a typical RV precision of 11-14 m s^{-1}.

3. Analysis and Results

3.1. Fit to the Subaru RV data alone

We determined the projected spin-orbit angle λ in several steps. First, in order to provide an independent determination, we use only the transit data from our new Subaru observations. Since those data alone are insufficient to determine all the Keplerian orbital parameters of the system, we also use the *out-of-transit* RV data points from OHP/SOPHIE Hébrard et al.

(2008). This essentially provides an independent determination of λ since we do not use the *in-transit* RV data from OHP/SOPHIE.

Our model for the RVs is similar in some respects to the previous analyses by Narita et al. (2009a) and Narita et al. (2010). Each RV data set (Subaru/HDS and OHP/SOPHIE) is modeled as

$$V_{\rm model} = K[\cos(f+\varpi) + e\cos(\varpi)] + \Delta v_{\rm RM} + \gamma_{\rm offset}, \tag{1}$$

where K is the orbital RV semi-amplitude, f is the true anomaly, e is the orbital eccentricity, ϖ is the angle between the direction of the pericenter and the line of sight, and finally γ is a constant offset for the data from a given spectrograph.

The velocity anomaly due to the RM effect $\Delta v_{\rm RM}$ is modeled with Equation (16) of Hirano et al. (2011). In order to compute $\Delta v_{\rm RM}$, we adopt the following values for the basic spectroscopic parameters; the macroturbulence dispersion $\zeta = 6.0$ km s^{-1}, the Gaussian dispersion (including the instrumental profile) $\beta = 3.0$ km s^{-1}, and the Lorentzian dispersion $\gamma = 1.0$ km s^{-1}. These values are taken from Gray (2005) and from the comparison with the numerical simulations by Hirano et al. (2011). Also, we assume the quadratic limb darkening law with $u_1 = 0.32$ and $u_2 = 0.36$ following Claret (2004).

We fit the two RV data sets (Subaru and OHP) by minimizing

$$\chi^2 = \sum_i \left[\frac{V_{\rm obs}^{(i)} - V_{\rm model}^{(i)}}{\sigma^{(i)}} \right]^2, \tag{2}$$

where $V_{\rm obs}^{(i)}$ is the observed RV value labeled by i while $V_{\rm model}^{(i)}$ corresponds to Equation (1). The uncertainty for each RV point is expressed by $\sigma^{(i)}$. Since we do not have any new photometric observations of the transit, we fix the photometrically measured parameters to be $R_p/R_s = 0.09057$, $a/R_s = 7.07$, and $i_o = 84.2^\circ$ from the refined parameter set by Winn et al. (2008). The remaining parameters are K, e, ϖ, $\gamma_{\rm offset}$ (for each data set), the rotational velocity of the star $v \sin i_s$, and the spin-orbit angle λ. We allow all the parameters to vary freely to minimize χ^2, using the AMOEBA algorithm. We add the stellar jitter of $\sigma_{\rm jitter} = 13.4$ m s^{-1} in quadrature to the RV uncertainties in Table 1 so that the reduced χ^2 in the global RV fitting becomes unity (after adding an additional parameter to allow for an offset between the two Subaru transits, as explained below). This jitter is accounted for in estimating the uncertainty for the system parameters in Table 2.

By fitting the Subaru/HDS data along with the out-of-transit OHP/SOPHIE data, we find the spin-orbit angle to be $\lambda = 36.7^\circ \pm 3.0^\circ$. This is in agreement with the previous finding by Winn et al. (2009), and in disagreement with the previous finding by Hébrard et al. (2008). The reduced chi-squared is $\tilde{\chi}^2 = 1.14$. Interestingly, when we plot the residuals between the Subaru/HDS data and the best-fit model, we find a small negative trend as a function of time over the 67-day span of the observations. To show this, we plot our new *out-of-transit* RV data as a function of BJD in the upper panel of Figure 1, along with the best-fit curve (red). The

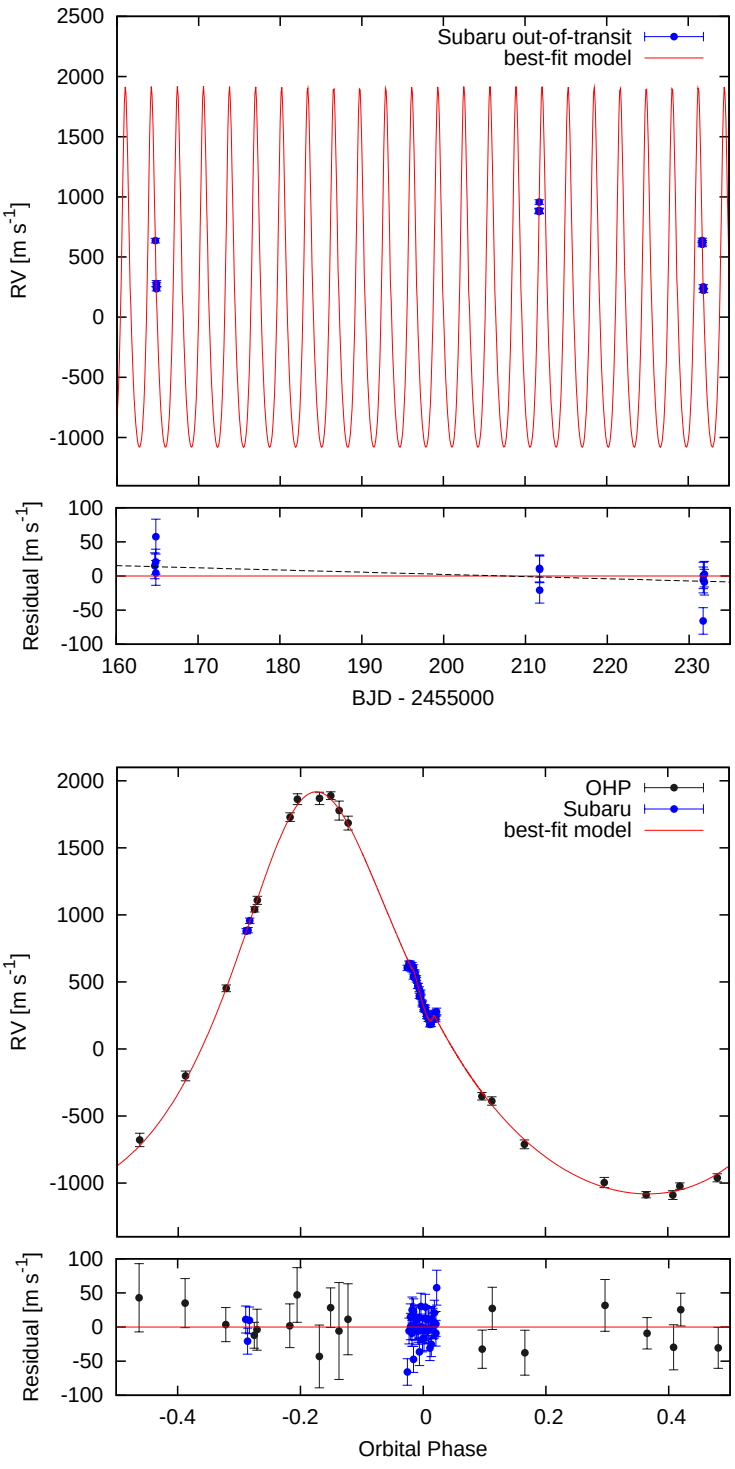

Fig. 1. (Upper) New RV data outside of transits, obtained with Subaru/HDS. The best-fit model curve is shown in red. The RV residuals at the bottom show a small negative trend in time. (Lower) The orbit of XO-3b based on the measurements with Subaru/HDS (blue), and the previously published RVs obtained with OHP/SOPHIE (black). For this figure, a linear RV trend ($\dot{\gamma}$) was fitted to the data and then subtracted. The best-fit model is shown as a red curve. The RV residuals are plotted at the bottom.

residuals from the best-fit curve are shown at the bottom. This trend cannot be corroborated or refuted by the previously published observations; the RV precision obtained by Johns-Krull et al. (2008) and Hébrard et al. (2008) was insufficient, and the precise RV measurements of Winn et al. (2009) did not cover a sufficiently long observation period.

This RV trend might indicate a possible additional body in the XO-3 system, but it is obviously premature to conclude so only with the 3 epochs of data. Future observations are needed. For the present purpose, in order to account for the offset in the overall RV between the different transit epochs, we introduced an additional model parameter $\dot{\gamma}$, representing a constant radial acceleration. We then refitted the Subaru RV data. The results from this fit are given in column (A) in Table 2. The uncertainty for each parameter is derived by the criteria that $\Delta\chi^2$ becomes unity. The inclusion of the constant acceleration improves the reduced chi-squared significantly ($\tilde{\chi}^2 = 0.91$ from 1.14 in the absence of $\dot{\gamma}$) and the best-fit RV acceleration is $\dot{\gamma} = -0.322 \pm 0.088$ m s^{-1} day^{-1}, indicating a 3.6σ detection. Since the two transit observations are separated by 67 days, the RV offset between the two transits is estimated as ~ 22 m s^{-1}. The resultant RVs as a function of the orbital phase are shown in the lower panel of Figure 1.

3.2. Joint fit to the Subaru and Keck data

Now that we have seen that our new results by Subaru/HDS support the previous RM measurement by Keck/HIRES (Winn et al. 2009), we would like to try to combine the two independent measurements (Subaru and Keck) and carry out a joint analysis in order to derive the parameters with greater precision.

We fit all of the transit data from Subaru/HDS and Keck/HIRES, and also the out-of-transit data from OHP/SOPHIE. We allow for a constant RV acceleration $\dot{\gamma}$, as before. We estimate the best-fit values for K, e, ϖ, $v \sin i_s$, λ, and $\dot{\gamma}$ as in Section 3.1. The results are summarized in the column (B) of Table 2. Most of the values are very close to the best-fit values in case (A). The projected rotation rate of $v \sin i_s = 18.4 \pm 0.8$ km s^{-1} is in good agreement with the spectroscopically measured value ($v \sin i_s = 18.54 \pm 0.17$ km s^{-1}, Johns-Krull et al. 2008). The resulting phase-folded RV anomalies during transits are plotted in Figure 2, in which the Keplerian motion and the linear RV trend are subtracted from the data. The RV data taken by Subaru/HDS are indicated in blue for the first transit and purple for the second transit, and those by Keck/HIRES are shown in green. The red solid curve is the best-fit curve based on the analytic formula of Hirano et al. (2011).

4. Discussion and Summary

We have investigated the RM effect for the XO-3 system, which was the first confirmed system with a significant spin-orbit misalignment (Hébrard et al. 2008). The new spectroscopic measurements including two full transits taken by Subaru/HDS and the new analysis method using the analytic formula for the RM effect by Hirano et al. (2011), found the spin-orbit angle

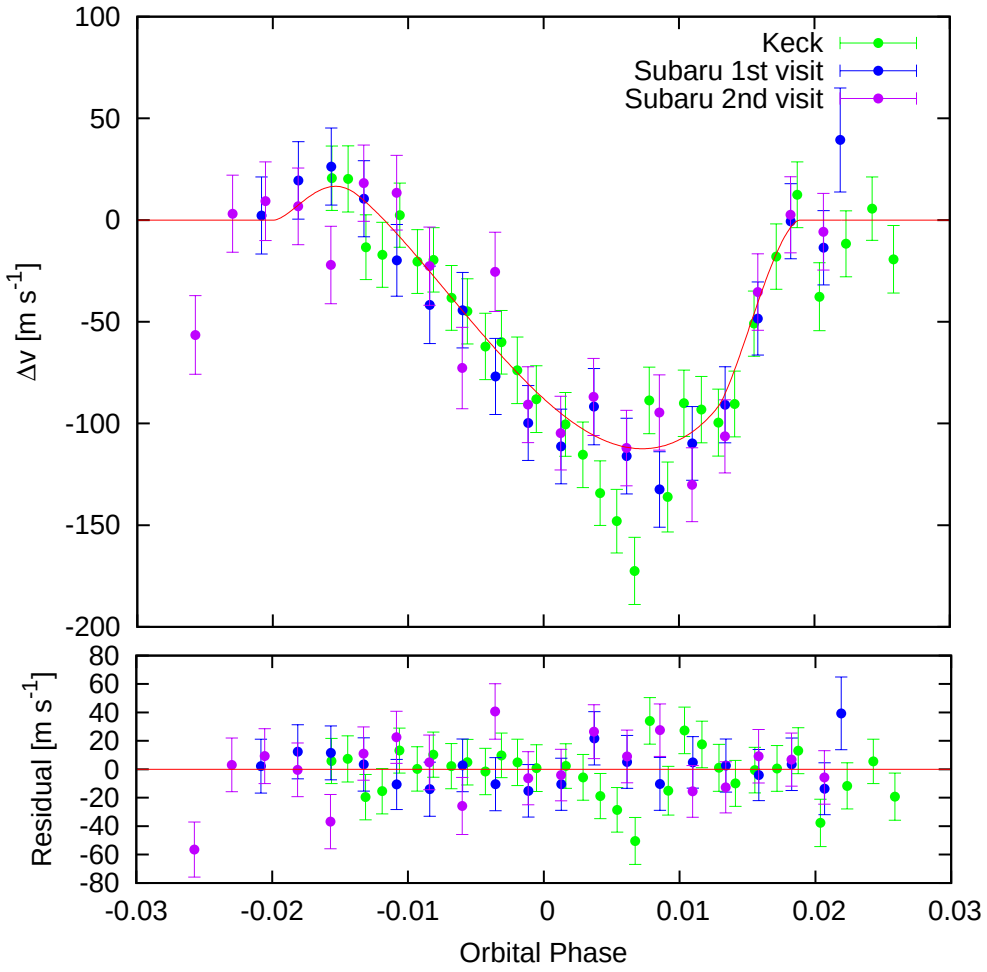

Fig. 2. RV data spanning the transit, after subtracting the orbital contributions to the velocity variation, and also a linear function of time. The plotted data includes the new Subaru/HDS data (blue for the fist transit on UT 2009 Nov. 29 and purple for the second transit on UT 2010 Feb. 4) and the previously published Keck/HIRES data taken on UT 2009 Feb. 2 (green). The RV residuals are plotted at the bottom.

of $\lambda = 37.3^\circ \pm 3.0^\circ$, supporting the result by Winn et al. (2009) based on the measurement with Keck/HIRES. The joint analysis of all the RV data sets covering three transits with Subaru/HDS and Keck/HIRES have shown that the projected stellar spin velocity estimated by the RM analysis well agrees with the spectroscopically measured value.

Our analysis also detected an RV trend, or at least RV offsets, among the three epochs of the Subaru/HDS observations. The cause of the extra RV variation is not clear. It is possibly an indication of a third body in the system: a stellar companion (binary), or an additional massive planet. Nevertheless it should be noted that this star is known to have a high "RV jitter" of around 15 m s^{-1}, and the precise physical causes and timescales of the jitter are not known. It is possible for starspots or other surface inhomogeneities being carried around by stellar rotation to produce a systematic offset in RV observations conducted on a single night.

Since the rotational velocity of the star is large for a planet-hosting star, even a relatively small spot could cause an apparent RV anomaly in a similar manner as the RM effect. For example, the RV acceleration of 22 m s^{-1} could be caused by a very dark spot whose size is only 0.002 of the total stellar disk area. The best way to investigate these possibilities is with additional measurements of the out-of-transit RV variation, with a precision better than 15 m s^{-1}.

As for the results for λ, we would like to understand the reason for the discrepancy between the OHP/SOPHIE results, and the Subaru/HDS + Keck/HIRES results. To this end we try several additional tests. As we have pointed out, Hébrard et al. (2008) employed the analytic formula based on the first moment of the distorted line profiles to describe the RM effect (Ohta et al. 2005). For rapidly rotating stars, however, the RM velocity anomaly computed from the first moment significantly deviates from that based on the cross-correlation method (Hirano et al. 2010). Therefore, we reanalyze the OHP data using the new analytic formula by Hirano et al. (2011) to see if the original estimate for the spin-orbit angle λ was biased. Instead of fixing the stellar spin velocity $v \sin i_s$ as done by Hébrard et al. (2008), we allow it to be a free parameter, and fit all the OHP RV data reported by Hébrard et al. (2008). The resulting spin-orbit angle is $\lambda = 58.8^\circ \pm 8.9^\circ$ and the stellar spin velocity of $v \sin i_s = 15.9 \pm 2.6$ km s^{-1}. The central value for λ approaches our new results ($37.4^\circ \pm 2.2^\circ$), but they still disagree with each other with $> 2\sigma$. This shows that a biased model played only a minor role in the discrepancy. The major reason seems to have been systematic effects in the OHP/SOPHIE dataset, perhaps due to the strong moonlight and high airmass that prevailed during their observations.

Incidentally, with only a small modification, the analytic formula by Hirano et al. (2011) can also be used to calculate the RM velocity anomaly in the presence of differential rotation (DR). The detection of DR would be of great interest for understanding the convective/rotational dynamics of the host star. Furthermore, it allows a possibility to break the degeneracy between the projected and the real three-dimensional spin-orbit misalignment angle by inferring the inclination angle of the stellar spin axis with respect to the line of sight (i_s), an angle that is ordinarily not measurable with the RM observations (if the star is a solid rotator).

Since XO-3 has a comparably large $v \sin i_s$, our new data may provide a good opportunity to search for the signature of DR, or at least to put constraints on the degree of DR quantitatively.

To model DR, we introduce two major parameters: the stellar inclination i_s and the coefficient of DR α. The stellar angular velocity Ω as a function of the latitude l on the stellar surface is written as

$$\Omega(l) = \Omega_{\rm eq}(1 - \alpha \sin^2 l), \tag{3}$$

where $\Omega_{\rm eq}$ is the angular velocity at the equator (Reiners 2003b). We step through a two-dimensional grid in α and $\cos i_s$, and for each grid point we fit the RVs with the six parameters

listed in Table 2. We compute the resulting χ^2 at each point (α, $\cos i_s$). We note here that the DR of our Sun is well described by $\alpha \simeq 0.2$. This also seems to be a typical value of other stars based on the spectral line analysis of (Reiners & Schmitt 2003a), although those authors also point out that some stars may have "anti-solar" like differential rotations in which $\alpha < 0$. (They could not distinguish these possibilities because of a degeneracy in the parameters describing the stellar line profile.) Thus, our grid extends from $-0.2 \leq \alpha \leq 0.2$ and $0 \leq \cos i_s \leq 0.95$. The case where $\cos i_s > 0.95$ is very unlikely because the star would need to be rotating unrealistically rapidly to give the observed value of $v \sin i_s$.

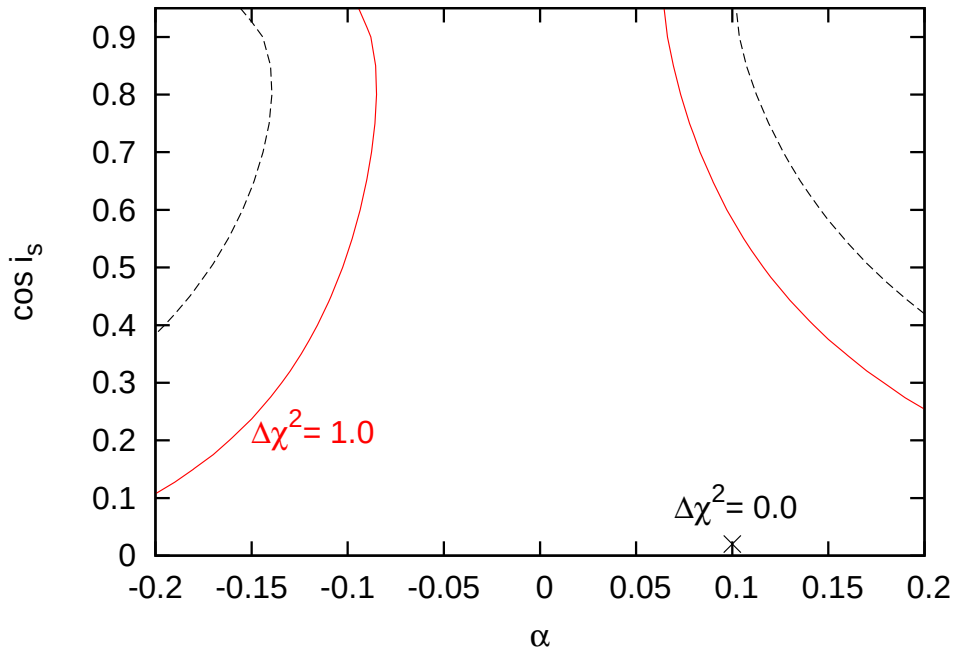

Fig. 3. Contour plot of $\Delta\chi^2$ in the space of the DR parameters α and i_s. The confidence region where $\Delta\chi^2 \leq 1.0$ is surrounded by the red solid curve. We also show the confidence boundary of $\Delta\chi^2 = 2.30$ by the black dashed line, which determines the 1σ region in a two-dimensional parameter space.

Figure 3 shows contours of $\Delta\chi^2 \equiv \chi^2 - \chi^2_{\rm min}$ in the (α, $\cos i_s$) plain. The location of the best-fit model (defining the condition $\Delta\chi^2 = 0.0$) is plotted with a black cross. This figure shows that with the current RV data, we are only able to provide fairly weak constraints on the parameters. We are able to rule out the far upper left and right corners of this parameter space, corresponding to Solar-like DR viewed at low inclination. We can rule out much stronger levels of DR ($|\alpha| \gtrsim 0.5$) regardless of orientation, but such strong levels of differential rotation are unlikely in any case.

The non-detection of DR may be ascribed to the large stellar jitter of the host star (15 m s^{-1}). This is often typical of relatively hot and rapidly rotating stars such as XO-3. The best cases for studying differential rotation through the RM effect would be somewhat cooler

stars that are still moderately rapid rotators ($\approx$ 5-10 km s^{-1}), for which a greater signal-to-noise ratio can be obtained.

We acknowledge the support for our Subaru HDS observations by Akito Tajitsu, a support scientist for the Subaru HDS. The data analysis was in part carried out on common use data analysis computer system at the Astronomy Data Center, ADC, of the National Astronomical Observatory of Japan. T.H. is supported by Japan Society for Promotion of Science (JSPS) Fellowship for Research (DC1: 22-5935). N.N. acknowledges a support by NINS Program for Cross-Disciplinary Study. J.N.W. acknowledges support from the NASA Origins program (NNX11AG85G) as well as the Keck PI Data Analysis Fund. M.T. is supported by the Ministry of Education, Science, Sports and Culture, Grant-in-Aid for Specially Promoted Research, 22000005. Y.S. gratefully acknowledges support from the Global Collaborative Research Fund (GCRF) "A World-wide Investigation of Other Worlds" grant and the Global Scholars Program of Princeton University.

References

Claret A. 2004, A&A, 428, 1001

Chatterjee, A., Sarkar, A., Barat, P., Mukherjee, P., & Gayathri, N. 2008, ApJ, 686, 580

Fabrycky, D., & Tremaine, S. 2007, ApJ, 669, 1298

Giménez, A. 2006, ApJ, 650, 408

Gray, D. F. 2005, The Observation and Analysis of Stellar Photospheres (3rd ed.; Cambridge University Press.)

Hébrard, G., et al. 2008, A&A, 488, 763

Hirano, T., et al. 2010, ApJ, 709, 458

Hirano, T., et al. 2011, ApJ, in press

Johns-Krull, C. M., et al. 2008, ApJ, 677, 657

McLaughlin, D. B. 1924, ApJ, 60, 22

Nagasawa, M., Ida, S., & Bessho, T. 2008, ApJ, 678, 498

Narita, N., et al. 2007, PASJ, 59, 763

Narita, N., et al. 2009a, PASJ, 61, 991

Narita, N., Sato, B., Hirano, T., & Tamura, M. 2009b, PASJ, 61, L35

Narita, N., et al. 2010, PASJ, 62, L61

Ohta, Y., Taruya, A., & Suto Y. 2005, ApJ, 622, 1118

Pont, F., et al. 2010, MNRAS, 402, L1

Queloz, D., Eggenberger, A., Mayor, M., Perrier, C., Beuzit, J. L., Naef, D., Sivan, J. P., & Udry, S. 2000, A&A, 359, L13

Reiners, A., & Schmitt, J. H. M. M. 2003, A&A, 398, 647

Reiners, A. 2003, A&A, 408, 707

Rossiter, R. A. 1924, ApJ, 60, 15

Sato, B., Kambe, E., Takeda, Y., Izumiura, H., & Ando, H. 2002, PASJ, 54, 873

Triaud, A. H. M. J., et al. 2010, A&A, 524, A25
Winn, J. N., et al. 2005, ApJ, 631, 1215
Winn, J. N., et al. 2008, ApJ, 683, 1076
Winn, J. N., et al. 2009, ApJ, 700, 302
Winn, J. N., Fabrycky, D., Albrecht, S., & Johnson, J. A. 2010a, ApJL, 718, L145
Wu, Y., Murray, N. W., & Ramsahai, J. M. 2007, ApJ, 670, 820

Table 1. A part of radial velocities measured with Subaru/HDS.

Time [BJD (TDB)]	Relative RV [m s^{-1}]	Error [m s^{-1}]
2455164.703174	523.9	13.4
2455164.711814	514.4	13.5
2455164.719564	497.3	13.4
2455164.727304	457.9	13.1
2455164.735054	404.1	11.5
2455164.742804	358.9	13.5
2455164.750544	333.2	12.8
2455164.758275	277.8	13.0
2455164.766005	232.3	12.7
2455164.773745	198.3	12.5
2455164.781485	195.7	13.1
2455164.789205	149.4	12.9
2455164.796945	111.1	12.8
2455164.804675	112.2	12.2
2455164.812405	109.7	13.0
2455164.820135	130.9	11.9
2455164.827875	157.7	12.7
2455164.835605	124.0	12.4
2455164.839555	166.4	21.8
2455211.720046	766.1	14.5
2455211.729516	774.0	13.7
2455211.738975	844.1	14.2
2455231.709440	492.8	14.0
2455231.718219	524.8	13.3
2455231.725949	506.8	13.9
2455231.733688	480.2	13.3
2455231.741418	427.6	13.5
2455231.749157	444.2	13.1
2455231.756887	416.1	12.5
2455231.764636	356.7	13.8
2455231.772366	283.6	14.9
2455231.780095	308.1	14.2
2455231.787834	220.1	13.0
2455231.795574	183.6	12.2
2455231.803313	179.2	13.4
2455231.811063	132.0	12.8
2455231.818802	127.6	12.8
2455231.826532	70.5	12.3
2455231.834271	72.9	12.0
2455231.842001	122.6	13.2

Table 2. The best-fit parameter sets.

Parameter	(A) Subaru	(B) Subaru + Keck
K [m s^{-1}]	1499.5 ± 9.9	1494.0 ± 9.5
e	$0.2859^{+0.0028}_{-0.0027}$	0.2883 ± 0.0025
ω [°]	347.4 ± 1.4	$346.1^{+1.2}_{-1.1}$
$v \sin i_s$ [km s^{-1}]	17.0 ± 1.2	18.4 ± 0.8
λ [°]	37.3 ± 3.0	37.4 ± 2.2
$\dot{\gamma}$ [m s^{-1} day^{-1}]	-0.322 ± 0.088	-0.320 ± 0.088
$\tilde{\chi}^2$	0.91	1.00 (fixed)